

# Preparation and Properties of $\text{Mn}_{1.5-x}\text{Cu}_x\text{Sb}$ and $\text{Mn}_{1.5-x}\text{Zn}_x\text{Sb}$ Solid Solutions with the *B8* Structure

M. Budzyński<sup>a</sup>, V. I. Mitsiuk<sup>b</sup>, V. V. Ryzhkovskii<sup>b</sup>, Z. Surowiec<sup>a</sup>, and T. M. Tkachenko<sup>b</sup>

<sup>a</sup> Institute of Physics, M. Curie-Skłodowska University, pl. M. Curie-Skłodowskiej 1, 20-031 Lublin, Poland

<sup>b</sup> Scientific–Practical Materials Research Centre, Belarussian Academy of Sciences,  
ul. Brovki 19, Minsk, 220072 Belarus

e-mail: lttt@physics.by

Received October 2, 2009

**Abstract**— $\text{Mn}_{1.5-x}\text{Cu}_x\text{Sb}$  ( $x \leq 0.30$ ) and  $\text{Mn}_{1.5-x}\text{Zn}_x\text{Sb}$  ( $x \leq 0.10$ ) solid solutions have been prepared using high-pressure high-temperature processing, and their structural and magnetic properties have been studied. The results of magnetic and Mössbauer measurements indicate that the interatomic magnetic interactions in the solid solutions are markedly weaker compared to those prepared by direct melting of elemental mixtures.

**DOI:** 10.1134/S0020168510100031

## INTRODUCTION

Manganese antimonide,  $\text{Mn}_{1+\delta}\text{Sb}$ , has a broad homogeneity range ( $0 \leq \delta \leq 0.30$ ) [1] and crystallizes in the *B8* structure (Fig. 1), in which the manganese atoms may occupy two structurally inequivalent sites: octahedral (MnI) and trigonal bipyramidal (MnII).  $\text{Mn}_{1+\delta}\text{Sb}$  has a net magnetic moment and, depending on the deviation from the equiatomic composition, may be a ferromagnet ( $\delta = 0$ ) or ferrimagnet ( $\delta > 0$ ). The manganese content of this compound has a significant effect on its physical properties. For example, with increasing  $\delta$  the temperature of its magnetic phase transition,  $T_C$ , drops from 600 to 300 K [2, 3]. Therefore, the possibility of varying the metal-rich boundary of this phase is of practical interest. Using high-pressure high-temperature processing, Ryzhkovskii and Goncharov [4] obtained *B8*-structure manganese antimonide with a manganese content as high as  $\delta = 0.50$ .

Mitsiuk et al. [5] prepared phase-pure solid solutions of copper and zinc in  $\text{Mn}_{1.10}\text{Sb}$ , which had the *B8* structure and a number of new properties [6]. The copper and zinc solubility in manganese antimonide was shown to be within 10 at % ( $\text{Mn}_{1.1-x}\text{M}_x\text{Sb}$  solid solutions with  $\text{M} = \text{Zn}$  or  $\text{Cu}$  and  $x \leq 0.10$ ).

In this paper, we report the preparation and properties of solid solutions of copper and zinc in  $\text{Mn}_{1.50}\text{Sb}$  ( $\delta = 0.50$ ). The solid solutions have the *B8* structure and a higher content of nonmagnetic components than in previous work [8]:  $\text{Mn}_{1.5-x}\text{Cu}_x\text{Sb}$  and  $\text{Mn}_{1.5-x}\text{Zn}_x\text{Sb}$  with  $x > 0.10$ .

## PREPARATION OF $\text{Mn}_{1.5-x}\text{Cu}_x\text{Sb}$ AND $\text{Mn}_{1.5-x}\text{Zn}_x\text{Sb}$ SOLID SOLUTIONS

To obtain solid solutions of copper and zinc in  $\text{Mn}_{1.5}\text{Sb}$ , we first prepared  $\text{Mn}_{1.5}\text{Sb}$  (1),  $\text{Mn}_{1.4}\text{Zn}_{0.1}\text{Sb}$  (2),  $\text{Mn}_{1.3}\text{Zn}_{0.2}\text{Sb}$  (3),  $\text{Mn}_{1.3}\text{Cu}_{0.2}\text{Sb}$  (4), and  $\text{Mn}_{1.2}\text{Cu}_{0.3}\text{Sb}$  (5) alloys by direct melting of elemental mixtures as described elsewhere [5]. Prior to synthesis, 2 at % manganese in the powder mixtures was replaced by an equivalent amount of the stable isotope  $^{57}\text{Fe}$  for Mössbauer measurements. The addition of such amounts of an isotope is common practice in Mössbauer spectroscopy and has no effect on the properties of solid solutions. It should, however, be kept in mind that the exact compositions of the solid solutions were

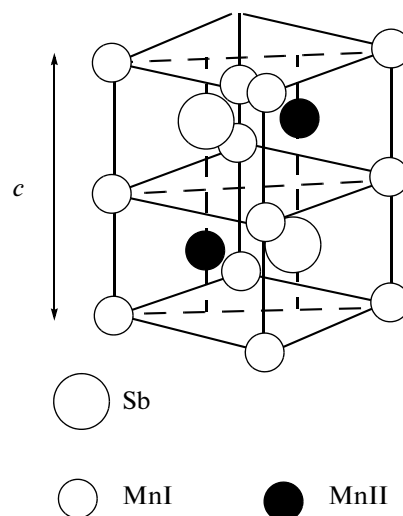


**Fig. 1.** Crystal structure of  $\text{Mn}_{1+\delta}\text{Sb}$ .

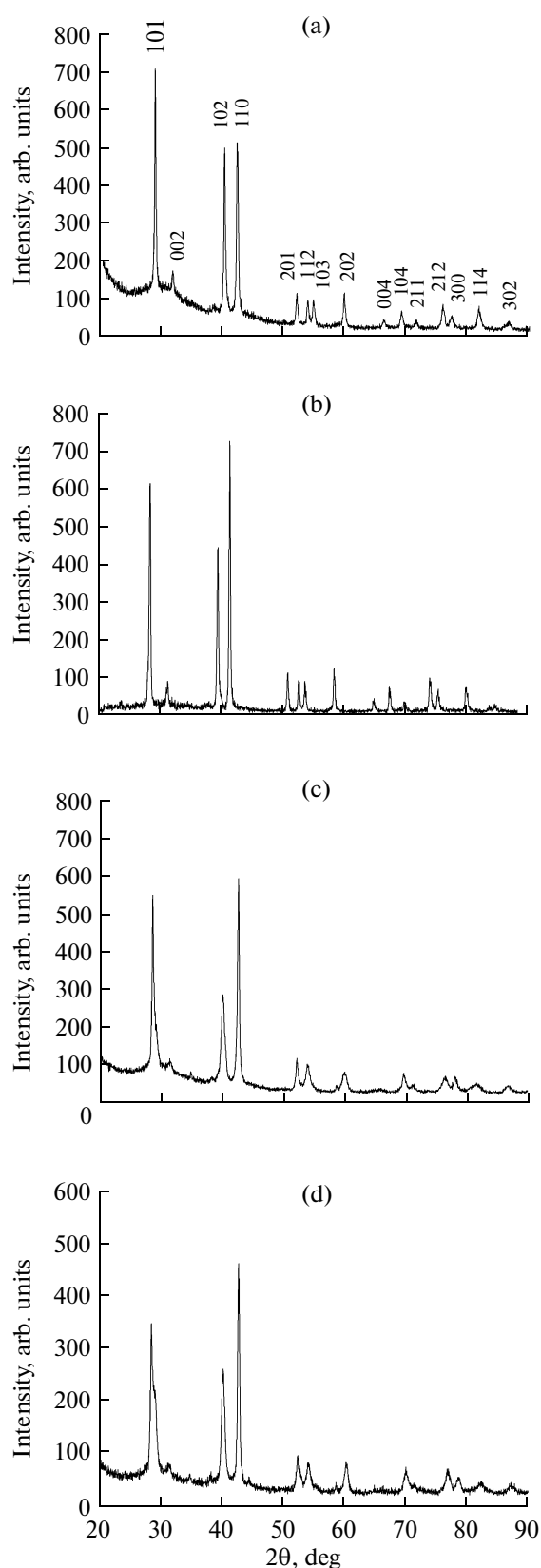


**Fig. 2.** X-ray diffraction patterns of the (a)  $\text{Mn}_{1.5}\text{Sb}$ , (b)  $\text{Mn}_{1.4}\text{Zn}_{0.1}\text{Sb}$ , (c)  $\text{Mn}_{1.3}\text{Cu}_{0.2}\text{Sb}$ , and (d)  $\text{Mn}_{1.2}\text{Cu}_{0.3}\text{Sb}$  solid solutions.

$\text{Mn}_{1.48}\text{Fe}_{0.02}\text{Sb}$  (1),  $\text{Mn}_{1.38}\text{Fe}_{0.02}\text{Zn}_{0.10}\text{Sb}$  (2),  $\text{Mn}_{1.28}\text{Fe}_{0.02}\text{Zn}_{0.20}\text{Sb}$  (3),  $\text{Mn}_{1.28}\text{Fe}_{0.02}\text{Cu}_{0.20}\text{Sb}$  (4), and  $\text{Mn}_{1.18}\text{Fe}_{0.02}\text{Cu}_{0.30}\text{Sb}$  (5). The alloys thus prepared were mixed-phase, as expected.

The alloys were then exposed to a constant quasi-hydrostatic pressure of 7 GPa at 2300°C for 5 min, followed by water quenching. The X-ray diffraction patterns of the resultant solid solutions are presented in Fig. 2 (the data were analyzed by the Rietveld method using FullProf software [7]).

The high-pressure high-temperature processing was found to raise the copper solubility in manganese antimonide with the *B8* structure, whereas the zinc solubility was insensitive to the synthesis procedure. In the X-ray pattern of the  $\text{Mn}_{1.2}\text{Cu}_{0.3}\text{Sb}$  alloy, the 101 peak was asymmetric, which was interpreted as evidence that the hexagonal structure of the alloy was distorted. This leads us to conclude that 30 at % is the highest copper content of the manganese-antimonide-based solid solution. The zinc solubility in  $\text{Mn}_{1.5}\text{Sb}$ , 10 at %, is the same as that in  $\text{Mn}_{1.1}\text{Sb}$ , which is somewhat unexpected and requires additional experimental studies.

The structural parameters of our samples are listed in Table 1.

The alloys obtained at high pressure were metastable: heating to above 450 K caused the high-pressure phase to decompose.

### PROPERTIES OF THE SOLID SOLUTIONS

The magnetization of the  $\text{Mn}_{1.5-x}\text{M}_x\text{Sb}$  solid solutions was measured at temperatures from 77 to 700 K in a magnetic field of 688 kA/m by the Faraday method, which allowed small samples to be used. The results are presented in Fig. 3. Analysis of the magnetization curves for the Zn- and Cu-containing solid solutions in comparison with that for  $\text{Mn}_{1.5}\text{Sb}$  indicates that partial substitution of nonmagnetic copper and zinc for magnetic manganese does not reduce the magnetization or Curie temperature of the material. In contrast, the transition to the paramagnetic state in the zinc- and copper-containing samples occurs at a higher temperature compared to undoped manganese antimonide (Table 1, Fig. 3).

**Table 1.** Structural and magnetic parameters of  $\text{Mn}_{1.5-x}\text{Cu}_x\text{Sb}$  and  $\text{Mn}_{1.5-x}\text{Zn}_x\text{Sb}$  solid solutions

Material	$a$ , Å	$c$ , Å	$c/a$	$T_C$ , K
$\text{Mn}_{1.5}\text{Sb}$	4.281	5.648	1.319	230
$\text{Mn}_{1.4}\text{Zn}_{0.1}\text{Sb}$	4.302	5.656	1.315	260
$\text{Mn}_{1.3}\text{Cu}_{0.2}\text{Sb}$	4.236	5.674	1.339	350
$\text{Mn}_{1.2}\text{Cu}_{0.3}\text{Sb}$	4.243	5.671	1.337	450*

\* Hypothetical Curie temperature.

At temperatures above 400 K, all of the solid solutions had an appreciable residual magnetization, which was due to the decomposition of the metastable high-pressure phase and relaxation to the thermodynamically stable state.

To gain more detailed insight into the microstructure and magnetic structure of the solid solutions prepared using high-pressure high-temperature processing, they were characterized by Mössbauer spectroscopy at liquid-nitrogen (77 K) and room (293 K) temperatures in a transmission geometry. The gamma source used was  $^{57}\text{Fe}(\text{Rh})$ . The room-temperature Mössbauer spectra of the solid solutions are presented in Fig. 4, and their 77-K spectra, in Fig. 5. The parameters of the spectra, evaluated using the Recoil program, are listed in Table 2.

The room-temperature spectra of the high-pressure  $\text{Mn}_{1.5}\text{Sb}$  sample (Fig. 4a) and zinc-containing solid solutions show quadrupole split lines with no magnetic component. This correlates with the results of magnetic measurements, which indicate that the Curie point of these materials lies below room temperature. The room-temperature spectrum of the  $\text{Mn}_{1.2}\text{Cu}_{0.3}\text{Sb}$  solid solution can be represented by two quadrupole doublets and two magnetic sextets with small effective magnetic fields at  $^{57}\text{Fe}$  ( $H_{\text{eff}} \leq 4.8$  T). The relationship between the areas of the subspectra suggests that there are roughly equal percentages of atoms involved in magnetic and nonmagnetic interactions. This interpretation of the Mössbauer data is consistent with the results of magnetic measurements, which show that the measurement temperature (RT) lies within the temperature range of the transition to the paramagnetic state.

The 77-K spectra of manganese antimonide and the copper-containing solid solutions show a combination of two magnetically split subspectra, each corresponding to atoms involved in magnetic interactions and located in either trigonal bipyramidal or octahedral sites. The spectrum of the zinc-containing solid solution also comprises two subspectra, but there are both magnetic and paramagnetic components. In all of the solid solutions, the effective magnetic field at  $^{57}\text{Fe}$  at liquid-nitrogen temperature is no greater than 5.4 T.

It is of interest to compare the present Mössbauer data for the  $\text{Mn}_{1.5-x}\text{M}_x\text{Sb}$  ( $M = \text{Zn}, \text{Cu}$ ) solid solutions prepared by high-pressure high-temperature processing to those for  $\text{Mn}_{1.1-x}\text{M}_x\text{Sb}$  solid solutions prepared without such processing [8]. As shown by Mitsiuk et al. [8], the room-temperature spectra of the  $\text{Mn}_{1.1-x}\text{M}_x\text{Sb}$  ( $M = \text{Zn}, \text{Cu}$ ) solid solutions each comprise two sextets with different effective magnetic fields at  $^{57}\text{Fe}$ :  $\approx 6$  and  $\approx 8$  T. Based on neutron diffraction data [3], the lower field was attributed to atoms in

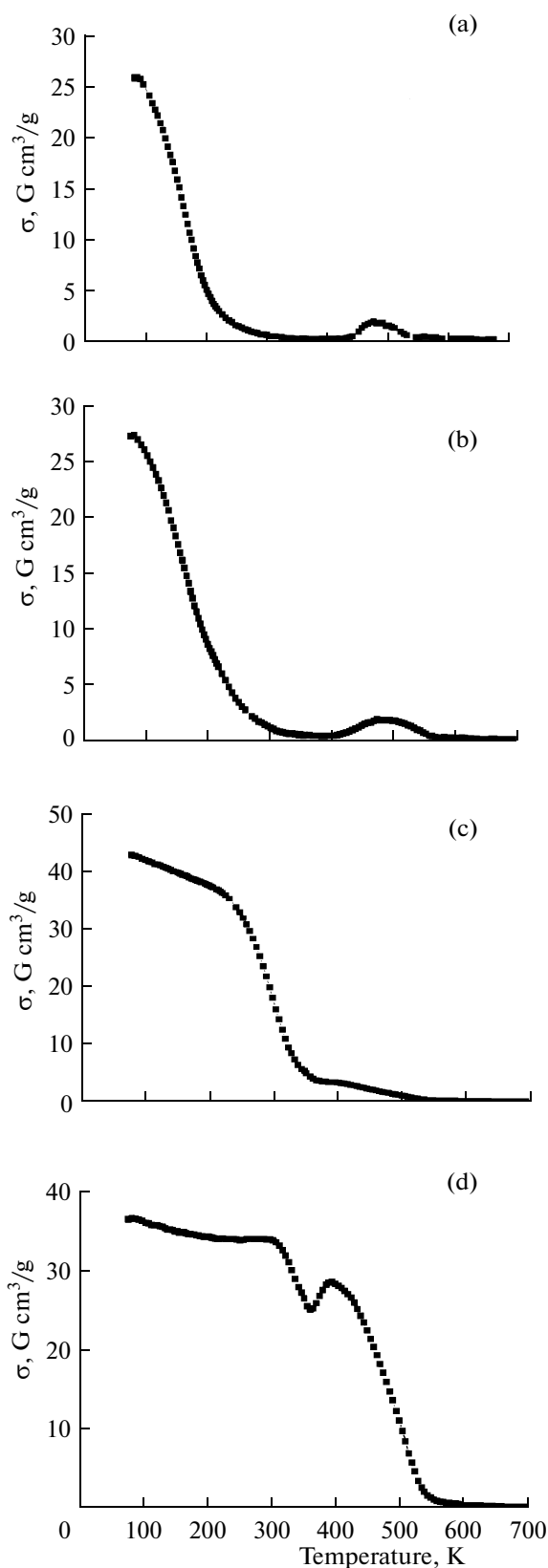


**Fig. 3.** Mass magnetization as a function of temperature for the (a)  $\text{Mn}_{1.5}\text{Sb}$ , (b)  $\text{Mn}_{1.4}\text{Zn}_{0.1}\text{Sb}$ , (c)  $\text{Mn}_{1.3}\text{Cu}_{0.2}\text{Sb}$ , and (d)  $\text{Mn}_{1.2}\text{Cu}_{0.3}\text{Sb}$  solid solutions.

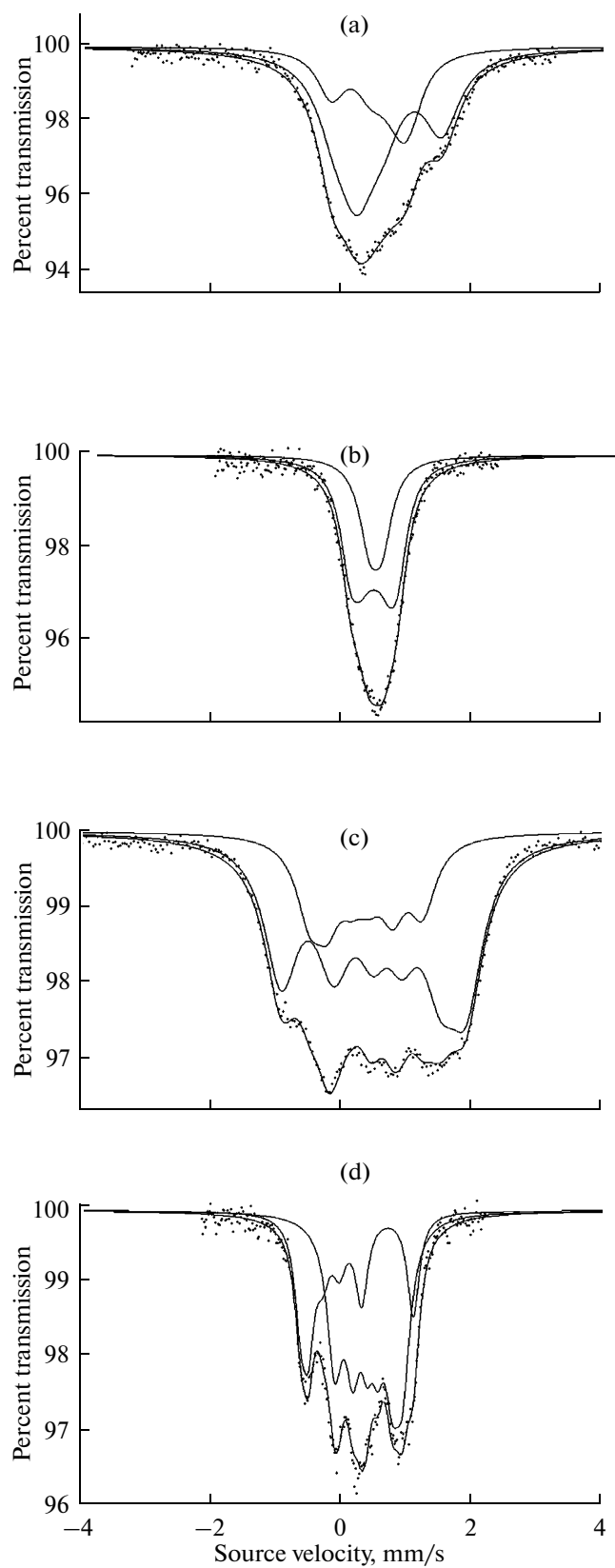


**Fig. 4.** Room-temperature Mössbauer spectra of the (a)  $\text{Mn}_{1.5}\text{Sb}$ , (b)  $\text{Mn}_{1.4}\text{Zn}_{0.1}\text{Sb}$ , (c)  $\text{Mn}_{1.3}\text{Cu}_{0.2}\text{Sb}$ , and (d)  $\text{Mn}_{1.2}\text{Cu}_{0.3}\text{Sb}$  solid solutions.

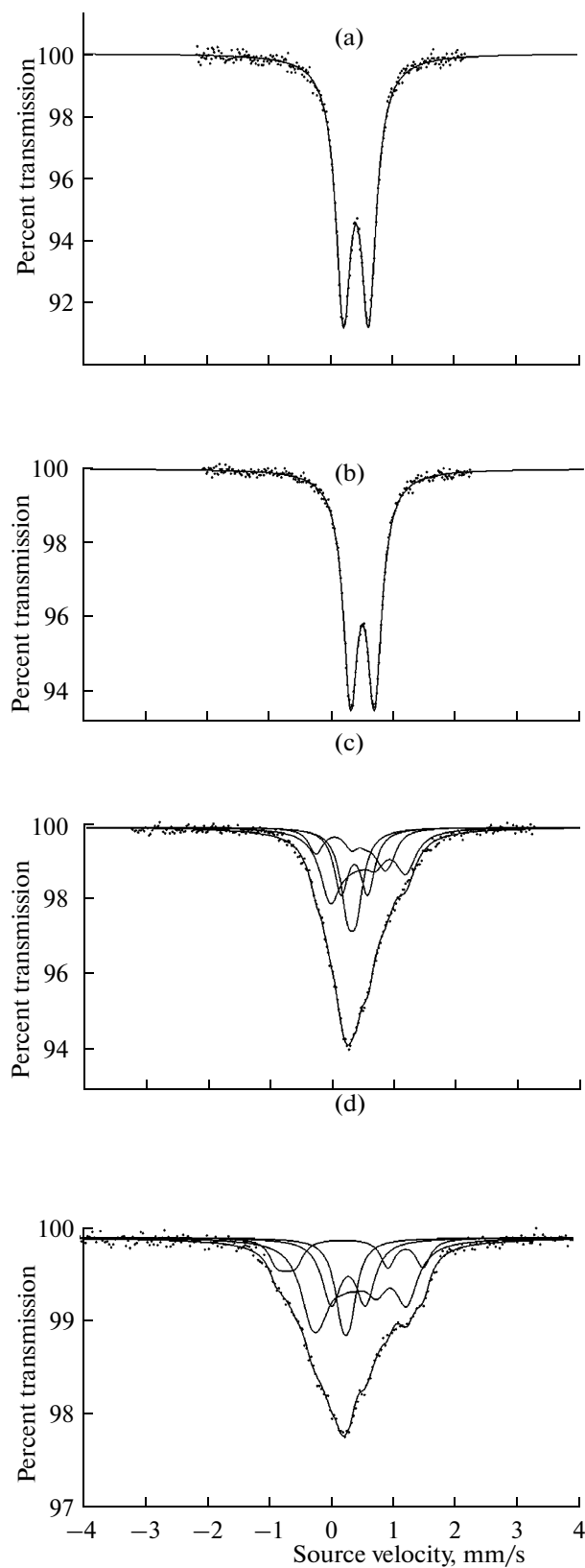


**Fig. 5.** 77-K Mössbauer spectra of the (a)  $\text{Mn}_{1.5}\text{Sb}$ , (b)  $\text{Mn}_{1.4}\text{Zn}_{0.1}\text{Sb}$ , (c)  $\text{Mn}_{1.3}\text{Cu}_{0.2}\text{Sb}$ , and (d)  $\text{Mn}_{1.2}\text{Cu}_{0.3}\text{Sb}$  solid solutions.

**Table 2.** Parameters of the  $^{57}Fe$  Mössbauer spectra of  $Mn_{1.5-x}Cu_xSb$  and  $Mn_{1.5-x}Zn_xSb$  solid solutions

Material	IS,	QS,	$H_{eff}$ , T	$\Gamma$ ,	IS,	QS,	$H_{eff}$ , T	$\Gamma$ ,	IS,	QS,	$H_{eff}$ , T	$\Gamma$ ,	IS,	QS,	$H_{eff}$ , T	$\Gamma$ ,
	mm/s	mm/s		mm/s	mm/s	mm/s		mm/s	mm/s	mm/s		mm/s	mm/s	mm/s		mm/s
	subspectrum I				subspectrum II				subspectrum I				subspectrum II			
	293 K								77 K							
$Mn_{1.5}Sb$	0.41	0.41	–	0.15					0.53	0.31	4.1	0.33	0.55	–0.18	3.4	0.25
$Mn_{1.4}Zn_{0.1}Sb$	0.41	0.39	–	0.15					0.28	0.20	–	0.18	0.26	–0.01	2.3	0.17
$Mn_{1.2}Cu_{0.3}Sb$	0.39	0.55	–	0.19	0.32	0.13	–	0.16								
	0.44	0.09	4.8	0.22	0.32	0.97	1.8	0.14	0.23	0.04	5	0.12	0.41	–0.02	3.2	0.14

Note: IS = isomer shift; QS = quadrupole splitting (relative to  $\alpha$ -Fe).

trigonal bipyramidal coordination, and the higher field, to atoms on the octahedral site.

It follows from the present Mössbauer results that the  $^{57}Fe$  field in the solid solutions depends significantly on the preparation procedure. In both the copper- and zinc-containing solid solutions prepared at high pressure, the  $^{57}Fe$  field is considerably lower than that in the alloys prepared by conventional melting, which attests to marked weakening of interatomic magnetic interactions. There are grounds to believe that this is contributed by the thermodynamically nonequilibrium state of the alloys processed at high pressure and temperature.

## CONCLUSIONS

High-pressure high-temperature synthesis of  $B8$  solid solutions of copper and zinc in manganese antimonide ensures an increase in copper content to 30 at % but does not increase the zinc content. The resultant solid solutions are metastable and decompose above 450 K.

The magnetic properties of the solid solutions (mass magnetization and Curie temperature) differ markedly from those of the parent  $Mn_{1.5}Sb$ .

Mössbauer results indicate that high-pressure high-temperature processing leads to weakening of interatomic magnetic interactions in the solid solutions of copper and zinc in manganese antimonide

compared to the solid solutions prepared by direct melting of elemental mixtures.

## REFERENCES

1. Teramoto, I. and Van Run, A.M.J.G., The Existence Region and the Magnetic and Electrical Properties of  $MnSb$ , *J. Phys. Chem. Solids*, 1968, vol. 29, pp. 347–355.
2. Sawatzky, E. and Street, B., The Structural Stability and Magneto-optical Properties of the NiAs Phase of the Manganese–Antimony System, *IEEE Trans. Magn.*, 1971, pp. 377–380.
3. Bouwma, J., van Bruggen, C.F., Haas, C., and van Laar, B., Neutron Diffraction and Magnetic Properties of  $Mn_{1+x}Sb_{1-y}Sn_y$ , *J. Phys. C*, 1971, vol. 32, pp. C1-78–C1-80.
4. Ryzhkovskii, V.M. and Goncharov, V.S., Effect of High-Pressure High-Temperature Processing on the Crystal Structure of  $Mn_{1+x}Sb$  ( $0 \leq x \leq 1.0$ ) Alloys, *Fiz. Tekh. Vys. Davlenii*, 2007, vol. 17, no. 2, pp. 53–58.
5. Mitsiuk, V.I., Ryzhkovskii, V.M., and Tkachenka, T.M., Structure and Magnetic Properties of  $MnSb(Zn)$  and  $MnSb(Cu)$  Solid Solutions, *J. Alloys Compd.*, 2009, vol. 467, nos. 1–2, pp. 268–270.
6. Mitsiuk, V.I., Ryzhkovskii, V.M., and Tkachenko, T.M., Belarus Patent 11937, 2007.
7. McCusker, L.B., Von Dreele, R.B., Cox, D.E., et al., Rietveld Refinement Guidelines, *J. Appl. Crystallogr.*, 1999, vol. 32, pp. 36–50.
8. Mitsiuk, V.I., Ryzhkovskii, V.M., and Tkachenka, T.M., Effect of Cu and Zn Substitutions on  $MnSb$  Properties, *AIP Conf. Proc.*, 2008, vol. 1070, no. 1, pp. 64–68.